Ceramics-Silikáty 67 (3), 371-378 (2023)
www.ceramics-silikaty.cz doi: 10.13168/cs.2023.0037

OPTIMISATION OF THE HYDROXYAPATITE SURFACE AREA PREPARED USING A POROGEN RUBBER SUSPENSION

#AHMAD FADLI, SILVIA R. YENTI, WISRAYETTI, AGUNG PRABOWO, JUMIATI HASIBUAN, VALLERIN G.T. HERJAN, ANA ISNANI, RETWI RESTYANDA

Chemical Engineering Department, Engineering Faculty, Universitas Riau, Jl. HR. Soebrantras, Km. 12.5, Pekanbaru, 28293, Riau, Indonesia

#E-mail: fadliunri@yahoo.com

Submitted July 27, 2023; accepted August 28, 2023

Keywords: Hydroxyapatite, Latex, Porous, Precipitation, Empirical model

Hydroxyapatite has been widely used in the biomedical industry due to its biocompatibility, bioactivity, and stable properties. A novel approach to handling its particles with a high surface area quality is urgently required. Therefore, this study aims to determine an empirical model of the surface area of precipitation-derived hydroxyapatite particles prepared with latex as a pore-forming agent. The results showed that the porous hydroxyapatite's surface area increased along with the pH, latex volume, and latex drop rate. The empirical model obtained to control the surface area of porous hydroxyapatite particles of porogen latex is $y = 15.961A + 217.418B – 161.16C – 20.407AB + 13.193AC + 22.27BC – 122.47$ *with* $R^2 = 99.99$ *%.*

INTRODUCTION

Hydroxyapatite ($Ca_{10}(PO_4)_6(OH)_2$) is one of the most widely used calcium phosphates due to its excellent bio-compatibility, bioactivity [1], osteoconductivity, and non-toxic properties [2]. However, increasing interest in improving its surface area is essential for the optimal performance [3]. This will help support the development of additive manufacturing systems in the biomedical industry, such as drug delivery [4], coatings for bone implants [5], and microcarriers [6].

There are several methods used to synthesise hydroxyapatite, which include sonochemical [7], sol-gel [8], and wet methods [9]. The sonochemical method relies on chemical reactions sparked by powerful ultrasonic radiation. This process consistently yields nano-sized items and achieves flawless control over the morphology, porosity, and size [7]. The thin layer preparation process, also known as the sol-gel method, enables the production of a chemically homogeneous layer from the final product with a fine powder structure. The long stages of this process include hydrolysis, condensation, ageing or ripening, and drying [8]. Meanwhile, the wet method is the most popular approach for producing hydroxyapatite due to the very low risk of contamination during processing, which results in a high yield at a relatively low cost with no environmental impact [10]. The two levels of the wet approach are coprecipitation and precipitation. Additionally, precipitation is the most effective in producing hydroxyapatite [11].

The wet chemical precipitation process allows for the convenient synthesis of hydroxyapatite in large quantities. Furthermore, it is a simple method to obtain this naturally occurring mineral in various shapes. The several factors that play a role in this process include synthesis temperature, an initial pH value of the reagent's solutions, the ageing process, and porogen additions [12]. This study investigates parameters such as the pH value, latex volume, and latex addition rate.

The synthesis of porous hydroxyapatite materials is of considerable interest and is constantly being developed to explore new applications. Its mesostructured materials are formed by a combustion treatment or a chemical etching process after removing the framework. The mesostructured is referred to as a pore, which controls the surface area, pore size, and pore volume of hydroxyapatite [13]. The pores of hydroxyapatite can be formed by the addition of porogen, including Cetyltrimethylammonium bromide (CTAB) [14], chitosan [9], I-Dodecanethiol [15], and micrometric latex beads [16].

The main plantation that grows in tropical climates is natural rubber latex, a primary biopolymer consisting of polyisoprene and non-rubber components such as lipids, proteins, carbohydrates, and metal ions [17]. Latex can be considered a suitable choice for obtaining porous hydroxyapatite because it can be easily removed using chemical or heat treatments [16].

Webler et al. [16] reported that the coprecipitation method of synthesising hydroxyapatite could enhance the production of its particles. It was observed that a new porous structure could be improved when micrometric latex beads were added to the slurry, such as a porogen. The study produced hydroxyapatite with a surface area of more than 200 $m^2 \cdot g^{-1}$ and a porosity level of 70 %. Absalan et al. [9] report that it is possible to obtain hydroxyapatite particles using the precipitation method with chitosan as a porogen. It was observed that the porous nature of this naturally occurring mineral could be obtained at pH of 8, 9 and 10 with porogen levels of 0.1 g and 0.3 g. Furthermore, the increase in the pH and introduction of porogen enhance the surface area, pore diameter, and pore volume of the hydroxyapatite particles.

The surface area of porous hydroxyapatite particles was modelled using a 23 factorial design to develop an empirical model of the appropriate surface area for the synthesis [18], which was then evaluated using a 2^3 factorial design to determine the impact of the pH, latex volume, and drop rate of latex. Kehoe et al. [19] stated that hydroxyapatite was successfully synthesised using precipitation. It was observed that using the 2^3 factorial design in the data handling enables a quick and effective collection of variables that affected the response. The most significant variations are the reaction temperature, stirring speed, and ageing time. Arantes et al. [20] also used the 2^3 factorial design in the data analysis. This method controlled the shape and size of the nanoparticles. Using this same approach, it was possible to create an empirical mathematical model that allowed developing a surface response plot to test the artificial system.

This study reports on the synthesis of porous hydroxyapatite materials using natural rubber latex as an agent, and a precipitation method of the variable pH, latex volume, and drop rate of latex. The surface area was modelled to obtain an empirical model of the appropriate surface area. This was conducted to determine which variables influence the surface area of the porous hydroxyapatite particles.

EXPERIMENTAL

Materials

The following materials were used: eggshells from the Indonesian Local Market as the calcium ion source, diammonium hydrogen phosphate as the phosphate ion source $(NH_4)_2HPO_4$ (Merck, Jerman), latex with a dry rubber content (DRC) of 60 % and a density of 1.12 $g \cdot cm^{-3}$ as the porogen (Brataco Chemika, Indonesia), aquabidest (Water One, Indonesia), aquadest (Brataco Chemika, Indonesia), nitric acid (HNO_3) (Merck, Jerman), ammonium hydroxide (NH_4OH) (Merck, Jerman), and ammonium chloride (NH_4Cl) (Merck, Jerman).

Synthesis of the Hydroxyapatite

Based on the following reaction, hydroxyapatite was synthesised using the precipitation method:

$$10\,Ca(NO_3)_2 + 6\,(NH_4)_2H(PO)_4 + 8\,NH_4OH \rightarrow Ca_{10}(PO_4)_6(OH)_2 + 20\,NH_4NO_3 + 6\,H_2O \quad (1)$$

A solution of 100 mL of $Ca(NO_3)_2$ and latex were added dropwise into 100 mL of an $(NH_4)_2HPO_4$ solution at 37 ºC under constant stirring (300 rpm) until it ran out. The mixture was continually stirred without heating for 30 minutes. After precipitation was complete, the solution was aged for 24 h, washed, filtered, and dried in an oven at 110 °C for 5 h. The sample was calcined for 5 h at 600 °C to obtain a porous hydroxyapatite powder.

Characterisation of the Porous Hydroxyapatite Particles

The following techniques were used to study the porous hydroxyapatite powder: The specific surface areas were observed with the Brunauer-Emmett-Teller (BET) method. Furthermore, the mean pore size was estimated from the desorption branch of the nitrogen adsorption-desorption isotherms using the Barrett-Joyner-Halenda (BJH) method. The crystal size and degree of crystallinity were observed by X-ray Diffraction (XRD). The diameter and particle size distribution were discovered by a Particular Size Analyser (PSA). Finally, the size and morphological characteristics of the porous hydroxyapatite powder were observed by a Field Emission Scanning Electron Microscope (FESEM).

Hydroxyapatite Surface Area Model

The surface area of the resulting porous hydroxyapatite particles was examined using a 2^3 factorial design to determine the impact of the pH, latex volume, and drop rate of the latex and to develop an empirical model of the appropriate surface area for the synthesis using the Minitab program. Table 1 shows the design of the experiment (DOE) and the variables.

Table 1. Synthesis hydroxyapatite factorial design 2^k.

Variable	Unit	Low Level (-)	High Level (+)
pH	-	9	12
Latex Volume	mL	0.5	1.0
Drop Rate of Latex	$mL \cdot min^{-1}$	0.05	0.6

The empirical model is created based on the data analysis results by substituting meaningful values for the constants and coefficients in the equation.

RESULTS AND DISCUSSION

BET Analysis

The main characteristics of the porous hydroxyapatite material are the specific surface area, pore volume, and pore size [21]. This study uses the BET analysis to ascertain the effect of each variable on the specific surface area of the hydroxyapatite particles that is affected by a pH of 9 and 12.

According to Figure 1, the surface area for the porous hydroxyapatite particles at pH 9 and 12 ranges between 19.595 to 54.141 $m^2 \cdot g^{-1}$ and 42.498 to 60.331 $m^2 \cdot g^{-1}$, respectively. The optimal performance of the porous hydroxyapatite particles occurred at a pH value of 12, with a latex volume of 0.5 mL and a latex drop rate of 0.6 $mL \cdot min^{-1}$, yielding a surface area of 60.331 $m^2 \cdot g^{-1}$. pH 9 showed the lowest porous hydroxyapatite particle surface area value of 19.595 $m^2 \cdot g^{-1}$, with a latex volume of 0.5 mL and a latex drop rate of 0.6 $mL \cdot min^{-1}$. This supports the report, which stated that the surface area of the resulting porous hydroxyapatite particles increases with the pH [22].

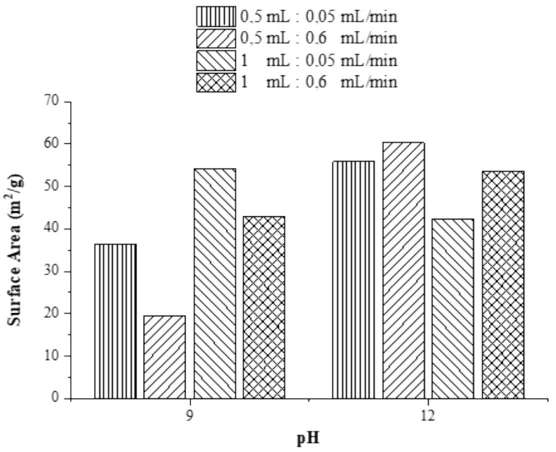

Figure 1. Relationship of the pH and the porous hydroxyapatite particle surface area.

The latex volume is one of the variables impacting the surface area of the porous hydroxyapatite particles. The latex used in this study was 0.5 mL and 1 mL. Figure 2 shows the relationship between the latex volume and the surface area of the porous hydroxyapatite particles. The results showed that latex as a porogen could improve the surface area [13]. This is because it expands and dissolves after calcination (burning temperature of 600 °C), which occurs during the synthesis of hydroxyapatite, thereby forming pores [16]. The addition of latex increases the surface area from 0.5 mL to 1 mL at pH 9. However, it was reduced by adding 1 mL latex at pH 12. This is because the resulting porous hydroxyapatite particles already have a high degree of purity. These results are consistent with research by Mohammad et al. [15], who reported that the surface area decreases when too much porogen is added, reaching the saturation point of the solution.

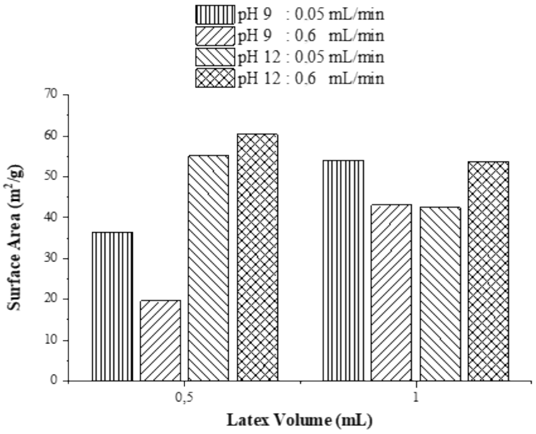

Figure 2. Relationship of the latex volume and the porous hydroxyapatite particle surface area.

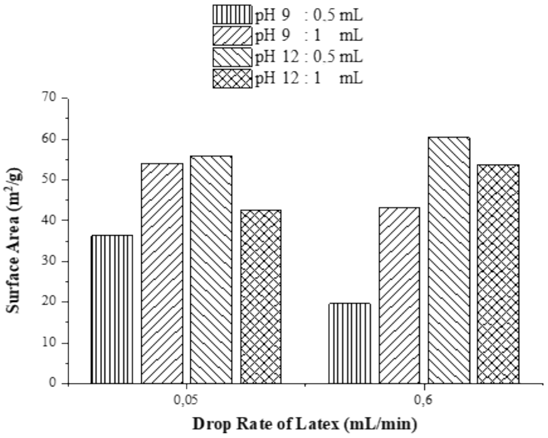

Figure 3. Relationship of the drop rate of latex and the porous hydroxyapatite particle surface area.

The latex drop rate modifies the surface area of the porous hydroxyapatite particles. This study used 0.05 and 0.6 $mL \cdot min^{-1}$ latex drop rates. Figure 3 shows that at pH 9, the highest latex drop rate could not increase the surface area of the porous hydroxyapatite particles. This was observed in the surface area of the porous hydroxyapatite particles, which is lower at a drop rate of latex of 0.6 mL/min, which is less than 0.05 $mL \cdot min^{-1}$. The addition of latex triggers an aggregation process at pH 9, leading to hydroxyapatite formation [14]. The surface area of the porous hydroxyapatite particles was increased at a pH of 12 when the drop rate of latex was enhanced from 0.05 mL·min^{-1} to 0.6 mL·min^{-1}.

BJH Analysis

The BJH (Barrett-Joyner-Halenda) analysis was used to determine the pore volume, size, surface area, physisorption isotherms, and hysteresis loops. Its base is the nitrogen adsorption-desorption isotherm. The nitrogen adsorption-desorption isotherm was utilised to examine the porosity of the sample with the largest surface area of hydroxyapatite particles at pH 12, latex volume of 0.5 mL, and drop rate of 0.6 mL·min^{-1}. According to the Barrett-Joyner-Halenda (BJH) analysis, the porous hydroxyapatite particles' pore size, volume, and surface area were 23.15 nm, 23.99 cm^3·g^{-1}, and 60.331 m^2·g^{-1}, respectively, which has a mesoporous type of pores. Meanwhile, there is a distinction between micropores (< 2 nm), mesopores (2 – 50 nm), and macropores (> 50 nm) [23]. According to Figure 4, the two nitrogen adsorption-desorption isotherm curves have the same type IV physisorption and type H3 hysteresis loops.

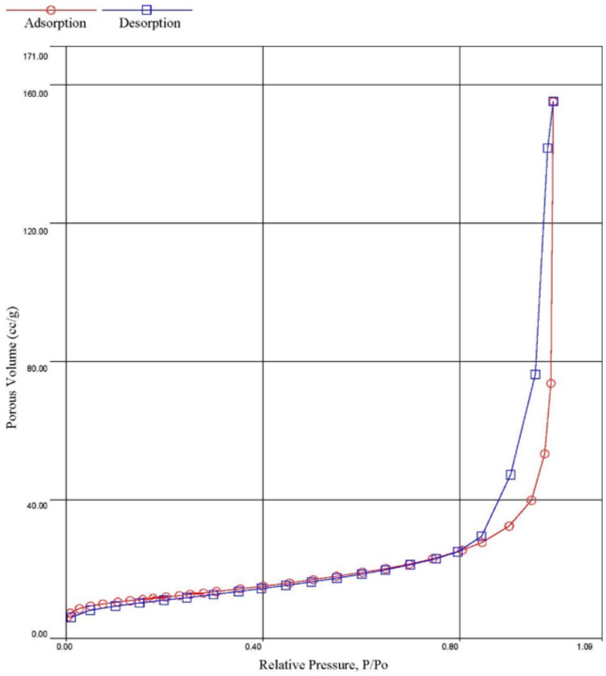

Figure 4. Nitrogen adsorption-desorption isotherm on the porous hydroxyapatite particles.

Porous Hydroxyapatite Particle Surface Area Model

In this study, the surface area of the porous hydroxyapatite particles was modelled to build an empirical model of the ideal surface area for the synthesis. Furthermore, 2^3 factorial design modelling was employed [18]. This approach was used to examine the surface area of the resulting porous hydroxyapatite particles to determine the impact of the pH, latex volume, and drop rate of latex. Table 2 shows the matrix design for the surface area parameters from the Minitab-19 software and the corresponding outcomes.

Table 2. Matrix design from the studied surface area results.

Treatment	Variable			Surface Area (m^2·g^{-1})
	pH	Latex Volume (mL)	Drops Rate of Latex (mL·min^{-1})	
1	9	1	0.6	43.051
2	9	1	0.05	54.141
3	12	1	0.05	42.498
4	9	0.5	0.6	19.595
5	12	0.5	0.6	60.331
6	9	0.5	0.05	36.385
7	12	0.5	0.05	55.916
8	12	1	0.6	53.739

The surface area results shown in Table 2 were statistically analysed using the Minitab-19 program. The response (y) to each variable condition can be predicted statistically using the model represented by Equation 2.

$$y = \beta_0 + \beta_1 x_1 + \beta_2 x_2 + \beta_3 x_3 + \beta_{12} x_1 x_2 + \beta_{13} x_1 x_3 + \beta_{23} x_1 x_3 + \beta_{123} x_1 x_3 \quad (2)$$

This was used to accurately forecast the surface area of the porous hydroxyapatite particles versus all the inputs.

The value of the coefficient of determination (R^2), which is in the range of 0 to 1, indicates the suitability of the statistical analysis outcome of the 2^3 factorial design. The R^2 value obtained was 99.99 %, as shown in Table 3. This suggests that the model has an excellent fit and can account for approximately 99.99 % of the parameters on the porous hydroxyapatite surface. Furthermore, the p-value for treatments A, B, AB, and AC is less than 0.05. The therapy significantly impacts the response when the p-value is less than 0.05, denoting a degree of significance. 0.05, or a p-value of 5 %, is used to base this. The factor influences the response while the p-value was above the threshold for significance (0.05), but it is not too significant [18]. The factors with the highest to lowest influence were in the order: AB, A, AC, B, BC, and C. Finally, the Pareto diagram in Figure 5 compared the greatest to the least effects.

Table 3. Estimation of the effects and coefficients on the surface area.

Term	Coefficient	P-Value
Constant	-122.47	0.002
A	15.961	0.012
B	217.48	0.034
C	-161.16	0.058
AB	-20.407	0.012
AC	13.193	0.016
BC	22.77	0.057

The empirical model that affected the resulting surface area of the porous hydroxyapatite particles was:

$$y = 15.961A + 217.48B - 161.16C - 20.407AB + 13.193AC + 22.77BC - 122.47 \qquad (3)$$

y is the surface area ($m^2 \cdot g^{-1}$), A is the pH, B is the latex volume (mL), and C is the drop rate of latex ($mL \cdot min^{-1}$). The parameter impact is quantified by the coefficient of -122.47, where a higher coefficient indicates a more substantial effect. The coefficient's sign indicates the direction of the effect. A positive sign indicates that the parameter increases along with the surface area. A negative sign shows that the surface area obtained decreases with an increase in the parameter [18].

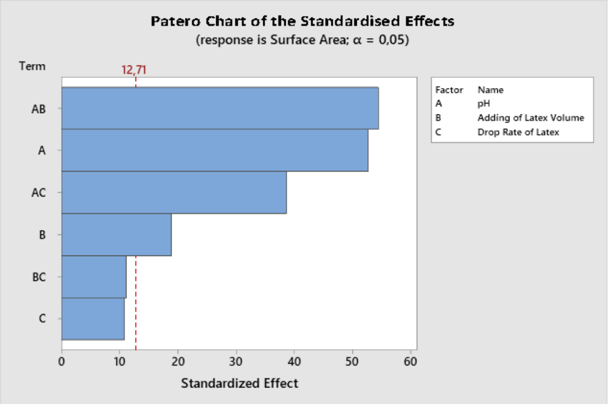

Figure 5. Pareto diagram on the surface area modelling of the porous hydroxyapatite particles.

According to the factorial matrix design, the 2^3 factorial matrix design shown in Figure 6, the anticipated surface area value of the porous hydroxyapatite particles is determined by entering the values of factors A, B, and C for each treatment. Figure 6 indicates that the experimental data and the data model have normal distribution [24]. Therefore, the developed empirical model significantly predicts the surface area of the porous hydroxyapatite particles and can be analysed by a regression model. This was demonstrated by the predicted R^2 result from the analysis of variance (ANOVA).

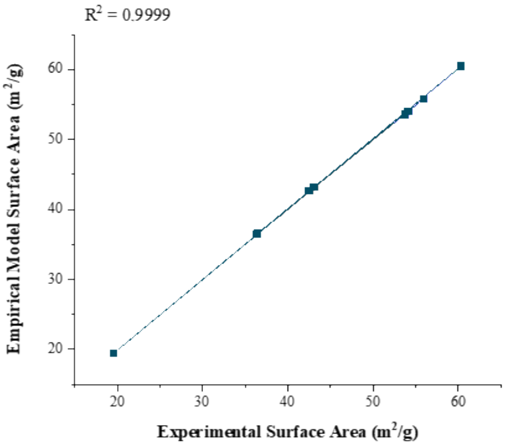

Figure 6. Comparison graph of the surface areas of the empirical model and the experimental surface area.

XRD Analysis

Figure 7 shows the XRD patterns of hydroxyapatite particles in treatment 5 with variations in the pH 12, latex volume of 0.5 mL, and drop rate of latex of 0.6 $mL \cdot min^{-1}$. The high peak at 2θ is 25.825° and 31.0615°, indicating the presence of its compounds. The diffraction patterns of the samples agree with the standard structural model of single-phase hydroxyapatite in the International Centre for Diffraction Data (ICDD) database no 96-230-0274.

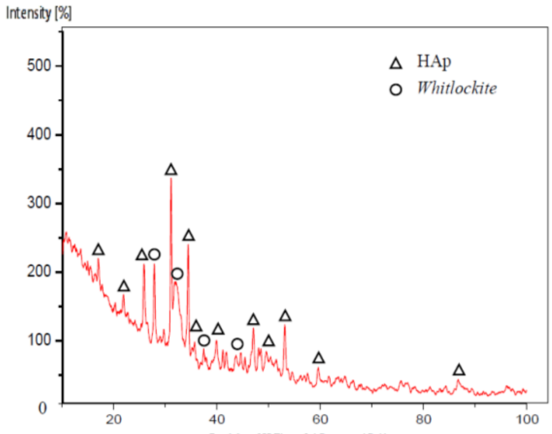

Figure 7. XRD patterns of the hydroxyapatite particles in treatment 5 with variation in the pH 12, latex volume 0.5 mL, and drop rate of latex 0.6 $mL \cdot min^{-1}$.

The crystallinity of this sample is relatively high and can be seen from the narrow and sharp diffraction peaks. The porous hydroxyapatite crystallinity calculated using the FWHM (Full Width at Half Maximum) parameter was 81.436 %, including an amorphous phase. Furthermore, the crystal size of the sample calculated using the Scherrer equation was 228.005 nm. The analysis also showed that there were two compounds formed, namely hydroxyapatite and β-tricalcium orthophosphate ($Ca_{18}Mg_2(HPO_4)_2(PO_4)_{12}$) or whitlockite. Magnesium is a compound that can trigger the formation of whitlockite. Finally, Mg^{2+} is one of the ions commonly discovered in natural rubber latex [25, 26].

PSA Analysis

According to Figure 8, the size of porous hydroxyapatite particle for treatment 4 with a variation of pH 9, latex volume of 0.5 mL, and drop rate of the latex of 0.6 mL·min^{-1}, is between 7.161 – 58.147 µm.

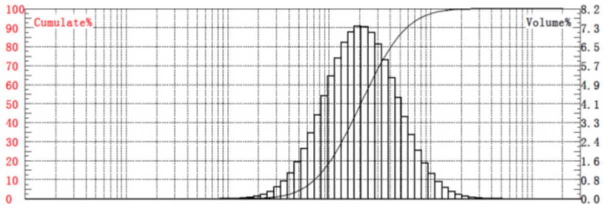

a) treatment 4 with a variation in the pH 9, latex volume 0.5 mL, drop rate of latex 0.6 mL·min^{-1}

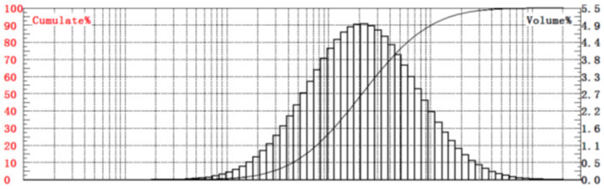

b) treatment 5 with a variation in the pH 12, latex volume 0.5 mL, drop rate of latex 0.6 mL·min^{-1}

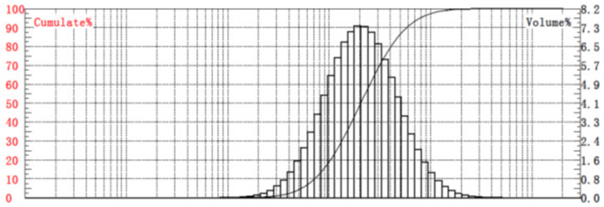

c) treatment 8 with a variation in the pH 12, latex volume 1 mL, drop rate of latex 0.6 mL·min^{-1}

Figure 8. Porous hydroxyapatite particle size.

Meanwhile, in Figure 8b, the particle size for treatment 5 with variations in the pH 12, latex volume of 0.5 mL, and drop rate of latex of 0.6 mL·min^{-1} is in the range of 4.431 – 101.005 µm. These results indicate that increasing pH can produce a larger particle size. This follows the report by [9], which stated that increasing the pH can elevate the particle size due to a rise in OH- ions.

According to Figure 8c, the particle size for treatment 8 with a variation in the pH 12, volume of latex of 1 mL, and drop rate of the latex of 0.6 mL·min^{-1} were in the range of 0.533 – 56.113 µm, which is smaller compared to treatment 5. These results conclude that the additional latex volume can reduce the hydroxyapatite particle size. This follows the research by [9], who stated that particle size decreases with the increasing chitosan concentration.

FESEM Analysis

Figure 9 shows the morphology of hydroxyapatite. It can be observed that the surface of the resulting hydroxyapatite particles contains several voids. The voids in the form of pores resulted from using latex as a pore-forming agent, which had been lost during the calcination process at a temperature of 600 °C. This follows the report by [16], who stated that during the calcination process, the latex particles started to melt and disappear at temperatures of 300 °C and above 500 °C, creating a space referred to as pores in the hydroxyapatite particles.

The morphology of the porous hydroxyapatite synthesised using the precipitation method with treatment 4 at pH 9, latex volume of 0.5 mL, and drop rate of latex of 0.6 mL·min^{-1}, is shown in Figure 9. It consists of various sizes, irregular needle-like shapes, and some voids.

According to Figure 9b, the sample synthesised with treatment 5 at pH 12, a latex volume of 0.5 mL, and a drop rate of the latex of 0.6 mL·min^{-1}, had a spherical-like shape, a larger particle size, and a wider space. This was also observed in the results of the BET analysis, which shows that this sample has the highest surface area. It can be seen from the comparison that the particle size increase along with the pH due to the rise in OH- ions [9].

Figure 9c shows the surface morphology of the porous hydroxyapatite particles synthesised by treatment 7 at pH 12, a latex volume of 0.5 mL, and a latex drop rate of 0.05 mL·min-1. It can be observed that the spherical-like particles are irregular and accumulate (aggregated) with smaller particle size and pore surface area when compared to the treatment sample 5 in Figure 9a. This is due to the rate of latex drops in treatment 7 is slower than in 5. It also follows the research conducted by Honglian et al. [14], who stated that this build up was due to its interaction with other substances during precipitation. The latex drop rate is directly proportional to the surface area of the porous hydroxyapatite particles [27].

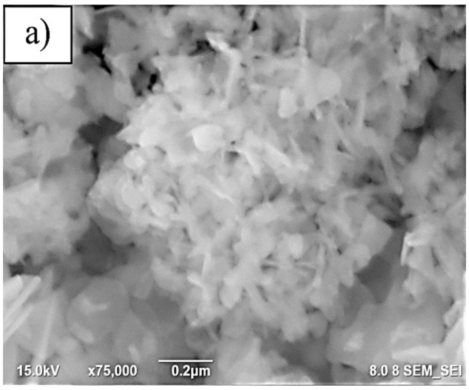

a) treatment 4 with a variation in the pH 9, latex volume 0.5 mL, drop rate of latex 0.6 mL·min^{-1}

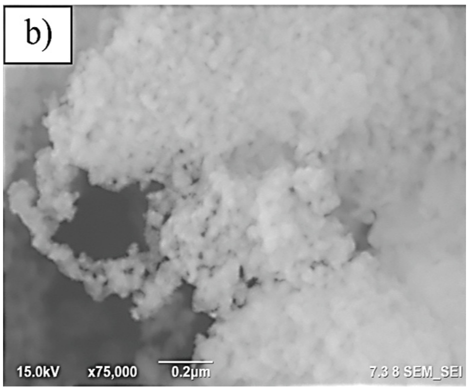

b) treatment 5 with a variation in the pH 12, latex volume 0.5 mL, drop rate of latex 0.6 mL·min^{-1}

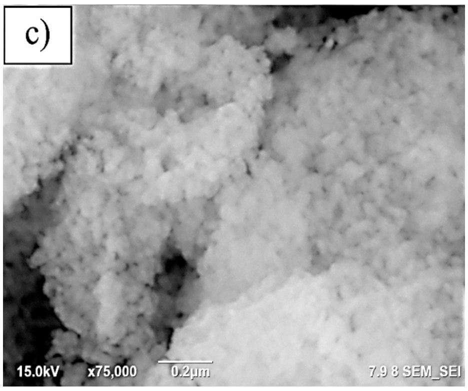

c) treatment 7 with a variation in the pH 12, latex volume 0.5 mL, drop rate of latex 0.05 mL·min^{-1}

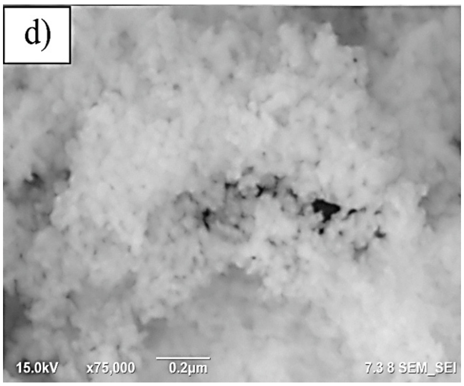

d) treatment 8 with a variation in the pH 12, latex volume 1 mL, drop rate of latex 0.6 mL·min^{-1}.

Figure 9. FE-SEM porous hydroxyapatite with 75,000x magnification.

Figure 9 shows that the overall morphology of the obtained porous hydroxyapatite is spherical, with a smaller particle size and surface area compared to the treatment sample 5 in Figure 9a. The addition of latex at pH 12 causes a decrease in the surface area of the sample. Since the hydroxyapatite particles produced already have good purity, the amount of latex (porogen) required will be less to produce an optimal surface area. This follows the research by Mohammad et al. [15], who stated that adding an excessive amount of porogen can cause a decrease in the surface area of the porous hydroxyapatite particles because it has reached the saturation point.

CONCLUSIONS

Natural rubber latex could be a good method to alter the surface properties of hydroxyapatite without modifying its crystalline structure. This new porous hydroxyapatite structure with a surface area of 60.331 m^2·g^{-1} was produced at pH 12, a latex volume of 0.5 mL, and a drop rate of latex of 0.6 mL·min^{-1}. The obtained empirical model to control the surface area of the particles with latex as porogen is $y = 15.961A + 217.418B - 161.16C - 20.407AB + 13.193AC + 22.27BC - 122.47$ with $R^2 = 99.99$ %. The order of parameters/variables from greatest to least influence include the pH and latex volume interaction (AB), pH (A), pH and drop rate of latex interaction (AC), latex volume (B), latex volume and drop rate of latex interaction (BC), and drop rate of latex (C).

Acknowledgments

The authors are grateful to the to the Education, Culture, Research, and Technology Ministry of the Indonesian Republic for the financial support under DRTPM Contract No. 157/E5/PG.02.00.PL/2023.

REFERENCES

1. György S., Károly Z., Fazekas P., Németh P., Bódis E., Menyhárd, A., et al. (2019): Effect of the reaction temperature on the morphology of nanosized HAp. *Journal of Thermal Analysis and Calorimetry, 138*, 145-151. doi: 10.1007/s10973-019-08255-z
2. Wojasiński M., Duszyńska E., Ciach T. (2015): Lecithin-based wet chemical precipitation of hydroxyapatite nanoparticles. *Colloid and Polymer Science, 293*, 1561-1568. doi: 10.1007/s00396-015-3557-0
3. Liu Z. L., Ji, Q. Y., Li X. D., Li S. P., Shen J., Lin J., Li D. X. (2020): Synthesis of hollow mesoporous HAp-Au/MTX and its application in drug delivery. *Colloids and Surfaces A: Physicochemical and Engineering Aspects, 586*, 124231. doi: 10.1016/j.colsurfa.2019.124231

4. Lara-Ochoa S., Ortega-Lara W., Guerrero-Beltrán C. E. (2021): Hydroxyapatite nanoparticles in drug delivery: physicochemistry and applications. *Pharmaceutics, 13*(10), 1642. doi: 10.3390/pharmaceutics13101642
5. Sari M., Kristianto N. A., Ana I. D., Yusuf Y. (2021): Carbonated Hydroxyapatite-based honeycomb scaffold coatings on a titanium alloy for bone implant application—Physicochemical and mechanical properties Analysis. *Coatings, 11*(8), 941.doi: 10.3390/coatings11080941
6. Kim T. W., Ahn W. B., Kim J. M., Kim J. H., Kim T. H., Perez R. A., Jang H. S. (2020): Combined delivery of two different bioactive factors incorporated in hydroxyapatite microcarrier for bone regeneration. *Tissue Engineering and Regenerative Medicine, 17*, 607-624. doi: 10.1007/s13770-020-00257-5
7. Fihri A., Len C., Varma R. S., Solhy A. (2017): Hydroxyapatite: A review of syntheses, structure and applications in heterogeneous catalysis. C*oordination Chemistry Reviews, 347*, 48-76. doi: 10.1016/j.ccr.2017.06.009
8. Szcześ A., Hołysz L., Chibowski, E. (2017): Synthesis of hydroxyapatite for biomedical applications. *Advances in Colloid and Interface Science, 249*, 321-330. doi: 10.1016/j.cis.2017.04.007
9. Absalan F., Sadjadi M. S., Farhadyar N., Sadr M. H. (2020): Synthesis of mesoporous hydroxyapatite with controlled pore size using the chitosan as an organic modifier: investigating the effect of the weight ratio and pH value of chitosan on the structural and morphological properties. *Journal of Inorganic and Organometallic Polymers and Materials, 30*(9), 3562-3573. doi: 10.1007/s10904-020-01623-5
10. Mazumder S, Nayak AK, Ara TJ, et al. (2018). *Hydroxyapatite Composites for Dentistry*. United Kingdom, Woodhead Publishing.
11. Agbeboh N. I., Oladele I. O., Daramola O. O., Adediran A. A., Olasukanmi O. O., Tanimola M. O. (2020): Environmentally sustainable processes for the synthesis of hydroxyapatite. *Heliyon, 6*(4), e03765. doi: 10.1016/j.heliyon.2020.e03765
12. Latocha J., Wojasiński M., Sobieszuk P., Gierlotka S., Ciach T. (2019): Impact of morphology-influencing factors in lecithin-based hydroxyapatite precipitation. *Ceramics International, 45*(17), 21220-21227. doi: 10.1016/j.ceramint.2019.07.103
13. Bakhtiari L., Javadpour J., Rezaie H. R., Erfan M., Shokrgozar M. A. (2015): The effect of swelling agent on the pore characteristics of mesoporous hydroxyapatite nanoparticles. *Progress in Natural Science: Materials International, 25*(3), 185-190. doi: 10.1016/j.pnsc.2015.06.005
14. Huang A., Dai H., Wu X., Zhao Z., Wu Y. (2019): Synthesis and characterization of mesoporous hydroxyapatite powder by microemulsion technique. *Journal of Materials Research and Technology, 8*(3), 3158-3166. doi: 10.1016/j.jmrt.2019.02.025
15. Mohammad,N. F., Amiruddin N. L., Saleh S. S. M., Taib M. A. A., Nasir N. F. M. (2019). Effect of swelling agent on pore properties of mesoporous carbonated hydroxyapatite. In *Journal of Physics: Conference Series* (Vol. 1372, No. 1, p. 012018). IOP Publishing. doi: 10.1088/1742-6596/1372/1/012018
16. Webler G. D., Rodrigues W. C., Silva A. E. S., Silva A. O. S., Fonseca E. J. S., Degenhardt M. F. S., et al. (2018): Use of micrometric latex beads to improve the porosity of hydroxyapatite obtained by chemical coprecipitation method. *Applied Surface Science, 436*, 141-151. doi: 10.1016/j.apsusc.2017.11.218
17. Sethuraj M. R., Mathew N. T. (1992). *Natural rubber: Biology, cultivation and technology*. Elsevier.
18. Freeman K. P., Cook J. R., Hooijberg E. H. (2021): Introduction to statistical quality control. *Journal of the American Veterinary Medical Association, 258*(7), 733-739. doi: 10.2460/javma.258.7.733
19. Kehoe S., Ardhaoui M., Stokes J. (2011): Design of experiments study of hydroxyapatite synthesis for orthopaedic application using fractional factorial design. *Journal of Materials Engineering and Performance, 20*, 1423-1437. doi: 10.1007/s11665-010-9704-3
20. Arantes T. M., Coimbra L. M., Cristovan F. H., Arantes T. M., Rosa G. M., Lião L. M. (2018): Synthesis and optimization of colloidal hydroxyapatite nanoparticles by hydrothermal processes. *Journal of the Brazilian Chemical Society, 29*, 1894-1903. doi: 10.21577/0103-5053.20180065
21. Melde B. J., Stein A. (2002): Periodic macroporous hydroxyapatite-containing calcium phosphates. *Chemistry of Materials, 14*(8), 3326-3331.doi: 10.1021/cm020259b
22. Neves J. G., Navarro da Rocha D., Lopes C. C., Prado da Silva M. H., Sinhoreti M. A. C., Correr-Sobrinho, L., et al. (2021): Effect of pH level and calcination on the production of calcium phosphates by acidic route of wet precipitation. *Cerâmica, 67*, 236-243. doi: 10.1590/0366-69132021673822965
23. Sing K. S. (1985): Reporting physisorption data for gas/solid systems with special reference to the determination of surface area and porosity (Recommendations 1984). *Pure and Applied Chemistry, 57*(4), 603-619. doi: 10.1351/pac198557040603
24. Nawawi M. (2020): Influence on service quality, product quality, product design, price and trust to xl axiata customer loyalty on students of PGRI karang sari belitang III oku timur vocational high school. *International Journal of Economics, Business and Accounting Research (IJEBAR), 4*(03), 1–13.
25. Pu'ad N. M., Koshy P., Abdullah H. Z., Idris M. I., Lee T. C. (2019): Syntheses of hydroxyapatite from natural sources. *Heliyon, 5*(5), e01588. doi: 10.1016/j.heliyon.2019.e01588
26. Karunanayake L., Perera G. P. (2006): Effect of magnesium and phosphate ions on the stability of concentrated natural rubber latex and the properties of natural rubber latex–dipped products. *Journal of Applied Polymer Science, 99*(6), 3120-3124. doi: 10.1002/app.22944
27. Smičiklas I., Onjia A., Raičević S. (2005): Experimental design approach in the synthesis of hydroxyapatite by neutralization method. *Separation and purification technology, 44*(2), 97-102. doi: 10.1016/j.seppur.2004.12.010